

Development of a Refractive Index Sensor Based on the Deposition of Gold and Silver Nanowires on ITO Glass for CA15-3 Detection

Zeng H*

School of Life Science and Technology, Harbin Institute of Technology, PR China

Abstract

As a step towards the development of highly sensitive and accurate biosensors for the early detection and monitoring of breast cancer, we have developed a refractive index sensor for the detection of CA15-3 breast cancer biomarker based on the deposition of gold and silver nanowires on ITO glass. 1 cm × 1 cm ITO glass was washed and vacuum dried. Gold films were sputtered on the clean dried ITO glass using an ion sputtering machine and labelled ITO/Au electrode. Silver nanowires solution were deposited on the ITO/Au electrode and labelled ITO/AU/AgNWs electrode. The ITO/Au/AgNWs electrode was then embedded in a 12 well-plate containing CA15-3 antibody and labelled ITO/Au/AgNWS/CA15-3 antibody electrode, which was used to detect CA15-3 antigen. The UV absorption wavelength of the sensor was found to be within the range of 320 nm to 350 nm. The sensor has a linear response to CA 15-3 antigen at concentrations ranging from 3 IU/mL to 32 IU/mL, and showed good CA15-3 detection properties with significant linear relationships between the wavelength change and the CA15-3 antigen concentration, the wavelength change and the refractive index, and the CA15-3 antigen concentration and refractive index. Our study provides a new and sure way towards the development of highly sensitive, accurate and efficient biosensors for the early detection and monitoring of breast cancer during therapy because Localized Surface Plasmon Resonance (LSPR) based detection techniques has an advantage over other detection techniques. Moreover, LSPR is superior to conventional methods when it comes to long term monitoring applications since LSPR of metallic nanoparticles do not bleach or blink. Also, the binding of nanoparticles to organic molecules increases the local refractive index since the index of refraction of typical buffer solutions are smaller than that of organic molecules.

Keywords: Refractive index; Breast cancer; Sensor; Cancer antigen 15-3

Introduction

Breast cancer is one of the leading causes of death in women worldwide. 22.9% of breast cancers in women were invasive as reported in 2008 by the International Agency for Research on Cancer, this resulted in the death of about 40,000 women worldwide [1].

Traditional methods such as Surgical Biopsy, Mammogram, and Fine Needle Aspiration Cytology are currently being used for the diagnosis of breast cancer [2]. Even though, some of these traditional methods have good breast cancer detection accuracy, they are very costly, varies widely, invasive and not readily available to all people [3]. Hence, there is the need for more effective and sophisticated methods that are less expensive, none invasive, and readily available to all people for the early diagnosis and treatment of breast cancer.

In recent years, nanotechnology has gained fresh impetus and has been used across several fields of science. Nanomaterials such as silver nanowires (AgNWs), silver nanoparticles (AgNPs), gold nanoparticles (AuNPs), quantum dots (QDs), magnetic nanoparticle (MNPs), carbon nanotubes (CNTs), among others, have been used to fabricate biosensors. For instance; developed an electrochemical biosensor based on Gold Nanoparticles Doped CA15-3 Antibody and Antigen interaction for the detection of CA15-3 biomarker [4]. Elakkiyal et al. [5] also developed an optical biosensor for the detection of CA15-3 biomarker using cadmium sulphide quantum dot (Cds-QD) in saline and serum samples spiked with antigen [5].

Due to its optical properties, ease of use as thin films, and good electrical conductivity, indium tin oxide (ITO) has gained so much attention and is one of the most commonly used transparent conductive oxides. It's properties has made it suitable for the development of biosensors [6,7].

In the quest for potent breast cancer biomarkers, a lot of attention has been focused on mucins. The MUC1 Tumor Marker, Cancer antigen 15-3 (CA 15-3) is overexpressed in greater than 90% of breast cancers and metastases [8,9]. The CA 15-3 level in blood has been reported to be 25–30 U/ml under normal conditions, but during malignancy, the level of CA 15-3 is increased depending on the stage of the disease [10,11]. CA 15-3 is an internationally accepted biomarker of breast cancer, the American Society of Clinical Oncology Panel, the National Academy of Clinical Biochemistry, and European Group on Tumor Markers Panel have recommended the use of CA 15-3 for monitoring the progress of therapy in patients with advanced breast cancer [12,13]. Hence, early detection of CA 15-3 is essential in diagnosis and prognosis of breast cancer.

There has been a higher interest and growth in optical biosensors, especially surface plasmon resonance based biosensors, because they have faster response, very high refractive index sensitivity, label free and real-time detection. This has made them more advantageous over conventional biosensors [14]. Localized surface plasmon resonance (LSPR) properties are determined by the size, shape and constituents of the nanoparticles, as well as the surrounding medium's index of refraction. With regards to the connection between LSPR and the factors

***Corresponding author:** Hongjuan Zeng, School of Life Science and Technology, Harbin Institute of Technology, PR China, Tel: 861582629368; E-mail: zenghj@uestc.edu.cn

Received: December 17, 2018; **Accepted:** February 11, 2019; **Published:** February 15, 2019

Citation: Zeng H (2019) Development of a Refractive Index Sensor Based on the Deposition of Gold and Silver Nanowires on ITO Glass for CA15-3 Detection. *J Nanomed Nanotechnol* 10: 523. doi: [10.4172/2157-7439.1000523](https://doi.org/10.4172/2157-7439.1000523)

Copyright: © 2019 Zeng H. This is an open-access article distributed under the terms of the Creative Commons Attribution License, which permits unrestricted use, distribution, and reproduction in any medium, provided the original author and source are credited.

that determine its properties, many researchers and scientists have shown keen interest in the development of highly sensitive biological and chemical biosensors based on nanomaterials [15-18]. The optical observation of individual nanoparticles that are as small as 20 nm and 30 nm in diameter for silver and gold respectively using a dark-field microscope is made possible by the high scattering of light derived from the LSPR of the noble metal nanomaterials [19]. This gives LSPR based detection techniques an advantage over other detection techniques.

Moreover, LSPR is superior to conventional methods when it comes to long term monitoring applications because LSPR of metallic nanoparticles do not bleach or blink. The binding of nanoparticles to organic molecules increases the local refractive index, since the index of refraction of typical buffer solutions are smaller than that of organic molecules. These results in a spectral redshift of the peak wavelength in both the scattering spectra and the extinction spectra [20-22]. Furthermore, additional enhancements can result from the interactions between nanoparticles. When the gap between the different particles becomes smaller, the coupling will become larger. That is, increasing inter-particle gap results in exponential coupling decay [23-26]. As a result of this, widely varied biological and chemical biosensors have been developed [27-29].

The index of refraction of a single cell is an essential biophysical property that has been measured and studied since the 1950s. Refractive index (RI) is an important parameter that varies among different intracellular organelles, and also among healthy and unhealthy or malfunctioned cells which leads to diseases that are severe [30]. Irregular shape, uneven chromatin texture, and increasing size of nuclear are some of the abnormalities found in cancer cells [31]. Cancer prognosis and diagnosis is becoming a reality based on these characteristics coupled with the continuous improving nanoscale diagnostic techniques [30]. In order to get a clear picture and a better understanding of the cycles of abnormal cells and the increased proliferation of cancer cells, many researchers have delved into refractive index studies of normal cells and cancer cells. According to previous research [32-34], the refractive index of most normal cells is 1.353 RIU whereas; the refractive index ranges from 1.370 to 1.400 RIU for cancer cells. An increase in RI may be connected to increased cell proliferation in cancer patients during various stages of cell cycles, since atypical cell cycles and increase in cell reproduction are shown in many human cancer cells. Spatial low-coherence quantitative phase microscopy was employed to measure the cell refractive indexes of specimen from breast biopsies [34]. The cells measured were; normal cells (healthy or non-cancerous cells), uninvolved cells (cancerous cells mistaken to be non-cancerous cells), and malignant cells (cancerous cells). According to their results, the refractive indexes of normal cells, uninvolved cells and malignant cells were 1.542, 1.544, and 1.545 RIU respectively. The increase in the nuclear refractive indexes from normal cells to malignant cells suggests that, nuclear refractive index might be a very important parameter for the diagnosis of cancer at early stages.

The effective refractive index of a single living cell was also measured using a microchip [35]. In their experiment, the five types of cancerous cells measured had their refractive indexes ranging from 1.392 to 1.401 RIU, which were larger than the refractive indexes of the normal cells which ranges from 1.35 to 1.37 RIU. Cancer cells have large refractive indexes than normal cells due to the large amount of protein in their nucleus, as a results of the rapid cell division during cancer [36]. In view of this, the effective refractive index of the cell can be used for early stage cancer detection before it becomes invasive.

Our work sort to design a refractive index sensor based on the

deposition of gold and silver nanowires for the detection of CA15-3. The materials, methods, results and discussion can be found in the subsequent sections of this paper. Even though more work need to be done to make the sensor sensitive and more accurate for clinical purposes, our work still showed promising statistics when compared to previously designed CA15-3 biosensors (Table 1).

Materials and Methodology

This section gives detailed information on some of the materials and reagents used in this research work. The preparation of the silver nanowires, gold plating of the ITO glass, the sensor fabrication process and the detection of CA15-3 antigen.

Materials

ITO glass was purchased from Szdiplay Company Limited (Shenzhen, China). CA15-3 antibodies and CA15-3 antigens standards, Phosphate buffer solution (PBS), Anhydrous ethanol ($\text{CH}_3\text{CH}_2\text{OH}$), Acetone ($\text{C}_3\text{H}_6\text{O}$), and Glycerin were purchased from Chengdu Kelong Chemical Reagent Factory (Chengdu, China). Potassium bromide (KBr), sodium chloride (NaCl), silver nitrate (AgNO_3) were purchased from Sigma-Aldrich Company Limited (Shanghai, China). Bovine Serum Albumin (BSA) and other chemicals used were of analytical grade. Silver nanowires (AgNWs) were prepared in our lab. All other chemicals used were of analytical grade. All commercially obtained chemicals were used as received without further purification. Also, all aqueous solutions were prepared using double distilled water.

Synthesis of AgNWs

Silver nanowires were made by the solution processing method known as the polyol process [37] with some modifications. First, 6.68 g of cysteine was added to 200 mL of ethylene glycol in a three necked round-bottom flask and stirred at 400 rpm using a magnetic stirrer. The mixture was then heated to a temperature of 170°C, and 0.1 g of potassium bromide (KBr), 0.2 g of sodium chloride (NaCl), and 2.793 g of silver nitrate (AgNO_3) were added to the solution and stirred at 200 rpm. The solution was then kept at 170°C for 4 hours to allow silver nanowires growth reaction to take place. The solution was then cooled to room temperature. The silver nanowire solution was filtered using a glass filter and centrifuged in order to get rid of particles that can reduce transmittance.

Gold plating

The gold-plated method was used to optimize the surface characteristics of the ITO conductive glass to make it more suitable for the fabrication of the CA 15-3 immunosensor. An SBC-12 ion sputtering apparatus was used to sputter gold films on the ITO conductive glass. The sputtering process is as follows:

- The clean-dried ITO conductive glass pieces were kept on the workbench of the ion sputtering apparatus, the machine and

Biosensor	Linear Range	Reference
ITO/Au/AgNWs/Ab	3 IU/mL – 32 IU/mL	Our work
AuNPs/Ab	5 U/mL - 75 U/mL	[4]
Cds QD/Cys/Ab	2 U/mL – 8 U/mL	[5]
RGO/Cus/screen-printed graphite electrode/CA15-3 antibody	1 U/mL – 150 U/mL	[38]
Gold electrode/streptavidin/anti-CA15-3 monoclonal antibody	50 – 15 x 10 ⁻⁶ U/mL	[39]

Table 1: Comparison of our work to previously prepared CA 15-3 antigen biosensors.

vacuum were turned on, and the vacuum was stabilized when the discharge current was within 10 mA.

- After the gold plating was completed, the glass slides were removed and the front part were marked and sealed to prevent contamination of the surface.

Measurements

Microscopic measurements were carried out using a biological microscope XSP-24 from Shanghai Batuo Instrument Company Limited, Shanghai, China. The microscope was connected to a computer with MW5CCD ScopePhoto software. To determine the morphological characteristics of the prepared silver nanowires, samples of the nanowires were placed under the microscope and clear images were captured on the computer with the aid of the MW5CCD ScopePhoto software and saved as BMP files. Measurements were also carried out for silver nanowires before and after centrifugation. Before making measurements, the software was calibrated and the objective lens used was indicated. A WAY-2S ABBE refractometer from Shanghai ShenGuang Instrument Company Limited (Shanghai, China) was used to check the refractive index of the 26% glycerin solution and CA15-3 antigen mixtures. The Magnetic stirrer was bought from Japan Nikon, PHS-W series PH meter from Shanghai Lida Instrument Factory was used to determine the pH of the various solutions, Electric blast drying oven 101-0 from Beijing Kewei Yongxing Instrument Company Limited. Ultrasonic Oscillator from Kunshan Ultrasonic Instrument Company Limited. An SBC-12 ion sputtering apparatus was used to sputter gold films on the ITO glass. Scanning Electron Microscope (SEM) JSM-6790LV from Japan Electronics Joel, A Hitachi U-2910 Double beam UV-Vis Spectrometer purchased from Hitachi High – Technologies Corporation (Tokyo, Japan) was used to characterize the modified electrodes

Sensor fabrication

Silver nanowires were deposited on the gold plated ITO glass (ITO/Au electrode) and labelled ITO/Au/AgNWs electrode. CA-153 antibody solution was kept in a 24-well plate. The ITO/Au/AgNWs electrode was then placed in the CA-153 antibody solution and incubated at 4°C for 48 hours to form ITO/Au/AgNWs/CA 15-3 antibody electrode. After the incubation, PBS was used to remove the unconjugated CA-153 antibody solution from the sensor's surface and placed in a 4°C freezer. The schematic illustration of the fabrication process is shown in Scheme 1.

Detection of cancer antigen 15-3 using the change of UV-visible spectrum as an indicator

The principle behind the sensors detection of CA 15-3 antigen is that, the CA 15-3 antibody on the sensors surfaces specifically binds to the CA 15-3 antigen. This bond between the Antibody and antigen results in the antigen binding to the surface of the sensors and thereby changing the optical properties of the sensor such as surface resistance, light absorption, mass transfer, among others. UV-Vis spectroscopy was used to characterize the changes in the optical properties of the biosensors after CA 15-3 antigen was introduced. The relationship between the changes in the optical properties of the sensors and the concentration of CA 15-3 antigen were discussed and the results showed a significant linear relationship between them. This means that the method used is essential in the detection of CA 15-3 antigen.

A series of glycerol solutions with different concentrations of CA-153 antigen were configured, and their refractive indexes measured using a refractometer. The glycerol solutions containing different concentrations of CA-153 antigen were loaded into a cuvette and

the sensor was kept inside the cuvette, the wavelength change of their characteristic absorption peaks were recorded with a UV-Vis spectrometer.

Results and Discussion

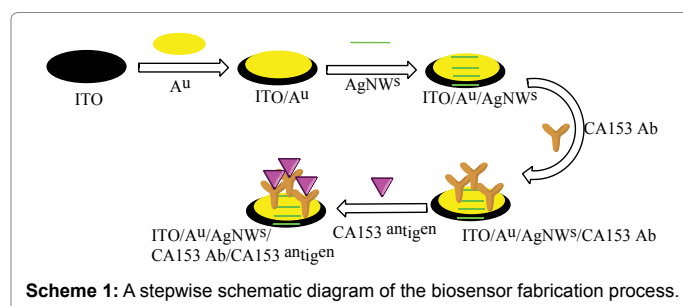
The above experiments were done several times until the desired results were obtained. Figure 1A and 1B represents microscopic views of silver nanowires before and after centrifugation. The silver nanowires in 1B have good aspect ratios and thin diameters than in 1A. Nanowires with thin diameters and good aspect ratios are considered to be of great quality. Hence, the centrifuged silver nanowires are of good quality than the un-centrifuged silver nanowires, since they have thin diameters and good aspect ratios than the un-centrifuged silver nanowires.

Pictures were taken before and after gold plating (Figure 2A and 2B). After gold plating, the ITO glass looked dense. Scanning electron microscopy was further done to ensure that the gold plating was successful. From Figure 3, the distribution of the gold films on the surface of the gold-plated ITO conductive glass is very uniform, indicating that the gold plating was successful.

The Ultraviolet visible absorbance spectrum of the various concentrations of CA 15-3 antigen with the sensor is illustrated in Figure 4. The optical properties of the sensor were altered after being exposed to the CA 15-3 antigen. This change is directly related to the amount of CA 15-3 antigen bounded to the surface of the sensor.

The gold (Au) film between the ITO conductive glass and the AgNWs enlarged the interaction between CA 15-3 antibody and CA 15-3 antigen, making it possibly to be detected. This increased the absorption intensity, which caused the CA 15-3 antigen to bind to the CA 15-3 antibody on the surface of the sensor, increasing the surface layer thickness and changing the sensor. The material distribution on the surface also increased the CA 15-3 antigen, which in turn increased the light absorption intensity. The UV absorption of the CA 15-3 was significantly magnified in the wavelength range of 320 nm to 350 nm, and with the increase of the CA 15-3 antigen content, the UV absorption peak wavelength shifts blue (decreased in wavelength with a corresponding increase in frequency) (Figure 4). Table 2 represents the CA15-3 concentration, RIs and the wavelength change of the sensor.

In other to determine whether there is a significant linear relationship between the change in the surface properties of the sensor and the concentration of CA 15-3, the wavelength change and the CA 15-3 concentration were analyzed. The correlation coefficient (R) and the calculated P-value are -0.99016 and 0.00117 respectively, indicating that there is a strong significant linear relationship between the change in the optical properties of the sensor and the CA 15-3 antigen concentration. As can be seen in Figure 5, the sensor has a linear response to CA 15-3 antigen at concentrations ranging from 3 IU/mL to 32 IU/mL, indicating that the constructed sensor is effective.



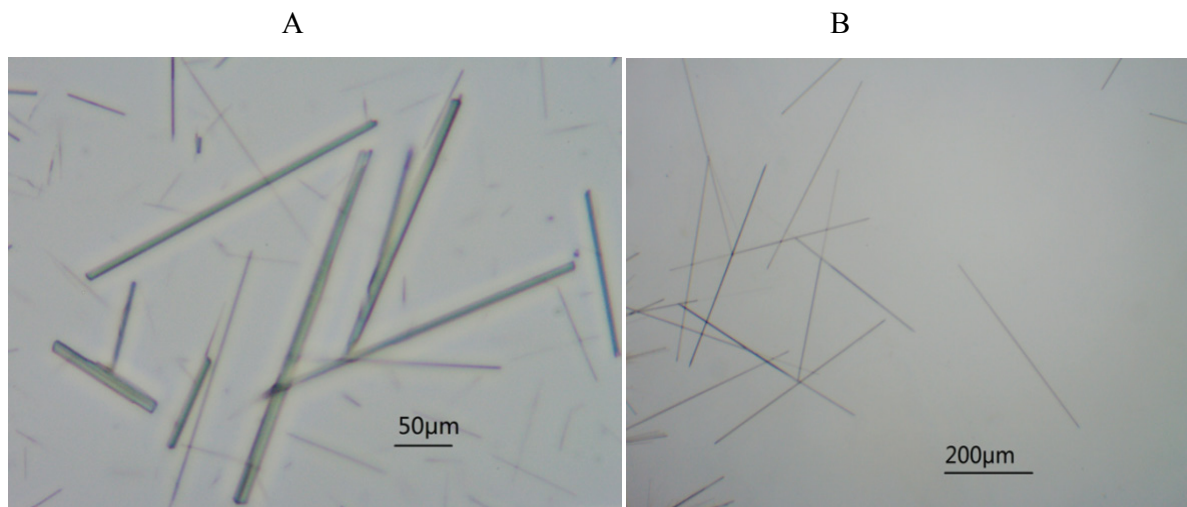


Figure 1: A: silver nanowires before centrifugation, B: silver nanowires after centrifugation.

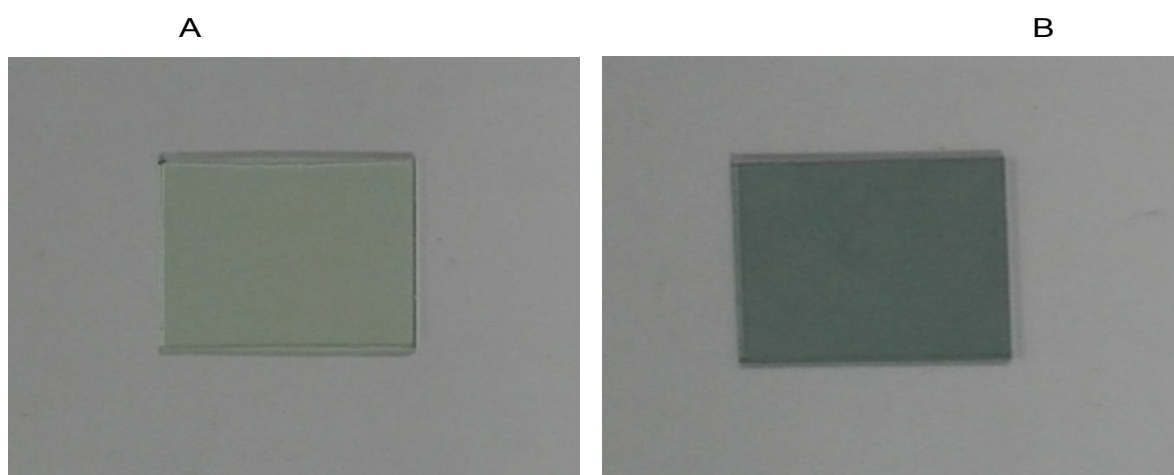


Figure 2: A: ITO glass before gold plating, B: ITO glass after gold plating.

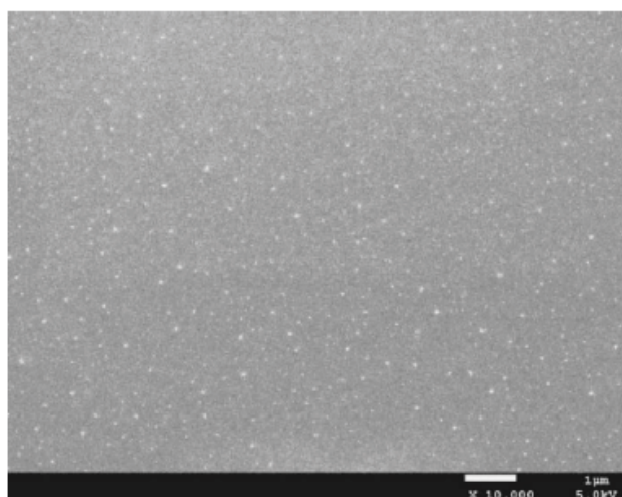


Figure 3: SEM image of gold plated ITO glass.

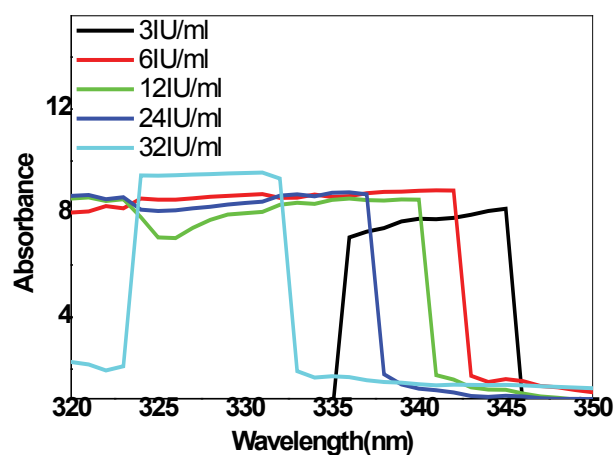


Figure 4: UV spectral response of the sensor to different concentrations of CA 15-3 antigen.

CA15-3 Concentration	RIs	Wavelength
3	1.3602	345
6	1.3595	342
12	1.3591	340
24	1.3588	336
32	1.3580	332

Table 2: Refractive indexes and wavelengths of different concentrations of CA 15-3 + glycerin solution.

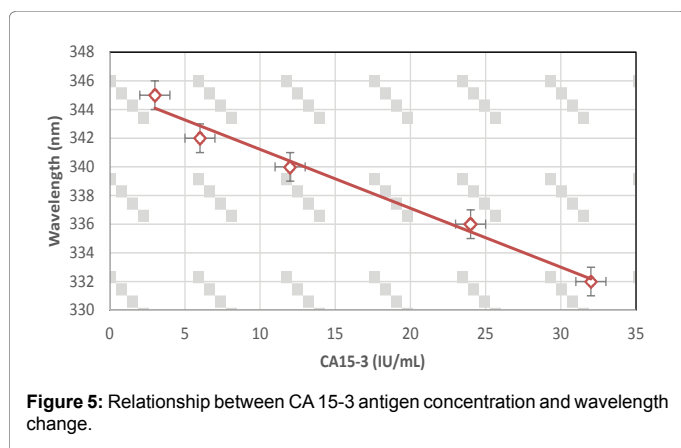


Figure 5: Relationship between CA 15-3 antigen concentration and wavelength change.

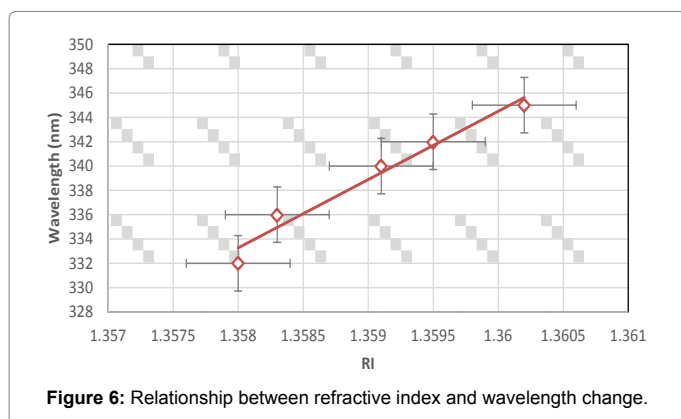


Figure 6: Relationship between refractive index and wavelength change.

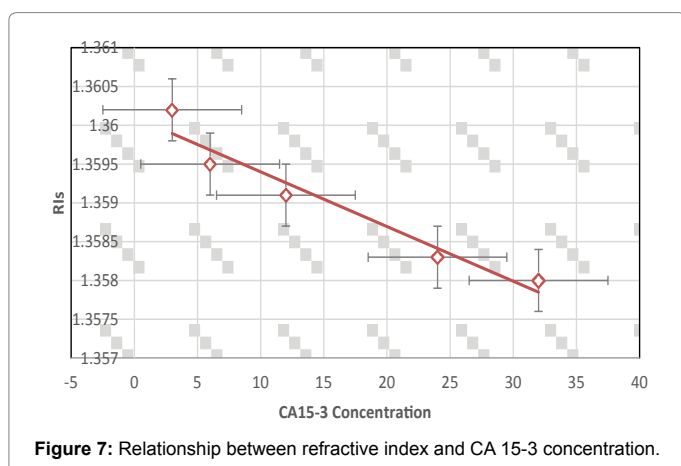


Figure 7: Relationship between refractive index and CA 15-3 concentration.

In order to determine whether there is a significant linear relationship between the change in the optical properties on the sensor's surface and the refractive index of the surrounding media, the

Wavelengths were plotted against the RIs. The relationship between the refractive index and the wavelength change is shown in Figure 6. The correlation coefficient and the calculated P-value are 0.98305 and 0.00264 respectively, indicating that there is a strong significant linear relationship between the change in the optical properties of the sensor's surface and the RIs.

We also determined the relationship between the refractive index and the CA 15-3 concentration (Figure 7). The correlation coefficient and the P-value are -0.97008 and 0.00618 respectively, indicating that there is a strong significant linear relationship between the refractive indexes and the CA 15-3 antigen concentration. The results show that, the sensor is valuable for the detection of CA 15-3, and suggests a new method which can be used to characterize the optical properties of the electrode surface.

Conclusion

The fabricated RI sensor responds to CA 15-3 antigen within the linear range of 3 IU/mL to 32 IU/mL, and within the wavelength range of 320 nm to 520 nm. Our work has laid a good foundation for the establishment of a simple, sensitive and portable RI biosensor for the detection of CA 15-3 antigen at the point of care and for monitoring the level of CA15-3 during therapy. Even though more experiments and optimizations are being done to further make the sensor highly sensitive for clinical setting, our work showed promising statistics when compared to other previously prepared CA 15-3 antigen biosensors. This method can also be used to fabricate sensors for the detection of other breast cancer biomarkers and cancers in general. More work can also be done to improve the sensor for the detection of multiple breast cancer biomarkers.

References

- Dheeba J, Wiselin Jiji G (2010) Detection of Microcalcification Clusters in Mammograms using Neural Network. *Int J Adv Sci Technol* 19: 13-22.
- Tang J, Rangayyan RM, Xu J, El Naqa I, Yang Y (2009) Computer-aided detection and diagnosis of breast cancer with mammography: recent advances. *IEEE Trans Inf Technol Biomed* 2: 236-251.
- Cedolini C, Bertozzi S, Londero AP, Bernardi S, Seriau L, et al. (2014) Type of breast cancer diagnosis, screening, and survival. *Clin Breast Cancer* 14: 235-240.
- Selwyna PGC, Loganathan PR, Begam KH (2013) Development of electrochemical biosensor for breast cancer detection using gold nanoparticle doped CA 15-3 antibody and antigen interaction. *Int Conf Signal Process Image Process. Pattern Recognit ICSIPR* 1: 1-7.
- Elakkiya V, Menon MP, Nataraj D, Biji P, Selvakumar R (2017) Optical detection of CA 15.3 breast cancer antigen using CdS quantum dot. *IET Nanobiotechnology* 11: 268-276.
- Yu C, Wang Q, Qian D, Li W, Huang Y, et al. (2016) An ITO electrode modified with electrodeposited graphene oxide and gold nanoclusters for detecting the release of H₂O₂ from bupivacaine-injured neuroblastoma cells. *Microchim Acta* 183: 3167-3175.
- Choudhary M (2013) Graphene Oxide based Label Free Ultrasensitive Immunosensor for Lung Cancer Biomarker. *J Biosens Bioelectron*.
- Senapati S, Das S, Batra SK (2010) Mucin-interacting proteins: From function to therapeutics. *Trends in Biochemical Sciences* 35: 236-245.
- Duffy MJ (2011) Prostate-specific antigen: Does the current evidence support its use in prostate cancer screening? *Annals of Clinical Biochemistry*.
- Bon GG, von Mensdorff-Pouilly S, Kenemans P, van Kamp GJ, Verstraeten RA, et al. (1997) Clinical and technical evaluation of ACS BR serum assay of MUC1 gene-derived glycoprotein in breast cancer, and comparison with CA 15-3 assays. *Clin Chem* 43: 585-593.
- Shao Y, Sun X, He Y, Liu C, Liu H (2015) Elevated levels of serum tumor markers CEA and CA15-3 are prognostic parameters for different molecular subtypes of breast cancer. *PLoS One*.

12. Duffy MJ (2006) Serum tumor markers in breast cancer: are they of clinical value? *Clin Chem* 52: 345-351.
13. Al-azawi D, Kelly G, Myers E, McDermott EW, Hill AD, et al. (2006) CA 15-3 is predictive of response and disease recurrence following treatment in locally advanced breast cancer. *BMC Cancer* 6: 220.
14. Cao J, Sun T, Grattan KTV (2014) Gold nanorod-based localized surface plasmon resonance biosensors: A review. *Sensors Actuators B Chem* 195: 332-351.
15. Sepúlveda B, Angelomé PC, Lechuga LM, Liz-Marzán LM (2009) LSPR-based nanobiosensors. *Nano Today*.
16. Chen Y, Ming H (2012) Review of surface plasmon resonance and localized surface plasmon resonance sensor? *Photonic Sensors*.
17. Jans H, Huo Q (2012) Gold nanoparticle-enabled biological and chemical detection and analysis. *Chemical Society Reviews*.
18. Luebert F (2010) *Nanoscience and Technology- A Collection of Reviews from Nature Journals*. Macmillan Publ Ltd World Sci Publ Co.
19. Arvizo RR, Bhattacharyya S, Kudgus RA, Giri K, Bhattacharya R, et al. (2012) Intrinsic therapeutic applications of noble metal nanoparticles. *Chemical Society Reviews* 7: 2943-2970.
20. Gu Z, Horie R, Kubo S (2002) Fabrication of a Metal-Coated Three-Dimensionally Ordered Macroporous Film and its Application as a Refractive Index Sensor. *Angew Chem Int Ed Engl*.
21. Lodewijks K, Van Roy W, Borghs G, Lagae L, Van Dorpe P (2012) Boosting the figure-of-merit of LSPR-based refractive index sensing by phase-sensitive measurements. *Nano Lett*.
22. Svedendahl M, Chen S, Käll M (2012) An introduction to plasmonic refractive index sensing. *Nanoplasmonic Sensors*.
23. Jain PK, Lee KS, El-Sayed IH, El-Sayed MA (2006) Calculated absorption and scattering properties of gold nanoparticles of different size, shape, and composition: Applications in biological imaging and biomedicine. *J Phys Chem B* 110: 7238-7248.
24. Schlather AE, Large N, Urban AS, Nordlander P, Halas NJ (2013) Near-field mediated plexcitonic coupling and giant Rabi splitting in individual metallic dimers. *Nano Lett*.
25. Schnell M, García-Etxarri A, Huber AJ, Crozier K, Aizpurua J, et al. (2009) Controlling the near-field oscillations of loaded plasmonic nanoantennas. *Nat Photonics*.
26. Taubert R, Ameling R, Weiss T, Christ A, Giessen H (2011) From near-field to far-field coupling in the third dimension: Retarded interaction of particle plasmons. *Nano Lett*.
27. Ghosh SK, Pal T (2007) Interparticle coupling effect on the surface plasmon resonance of gold nanoparticles: From theory to applications. *Chemical Reviews*.
28. Aćimović SS, Kreuzer MP, González MU, Quidant R (2009) Plasmon near-field coupling in metal dimers as a step toward single-molecule sensing. *ACS Nano*.
29. Song Y, Wei W, Qu X (2011) Colorimetric biosensing using smart materials. *Advanced Materials*.
30. Liu PY, Chin LK, Ser W, Chen HF, Hsieh CM, et al. (2016) Cell refractive index for cell biology and disease diagnosis: past, present and future. *Lab Chip* 16: 634-644.
31. Lu K, Lu L, Suresh S (2009) Strengthening materials by engineering coherent internal boundaries at the nanoscale. *Science*.
32. Liang XJ, Liu AQ, Lim CS, Ayi TC, Yap PH (2007) Determining refractive index of single living cell using an integrated microchip. *Sensors Actuators A Phys*.
33. Choi WJ, Jeon DI, Ahn SG, Yoon JH, Kim S, et al. (2010) Full-field optical coherence microscopy for identifying live cancer cells by quantitative measurement of refractive index distribution. *Opt Express*.
34. Wang P, Bista R, Bhargava R, Brand R, Liu Y, et al. (2013) Spatial-domain low-coherence quantitative phase microscopy for cancer diagnosis. *Opt Lett*.
35. Korean Sensors Society, Institute of Electrical and Electronics Engineers, IEEE Electron Devices Society (2005) *Transducers'05*: Seoul, Korea, the 13th International Conference on Solid-State Sensors, Actuators and Microsystems, digest of technical papers. Piscataway NJ.
36. Backman V, Wallace MB, Perelman LT, Arendt JT, Gurjar R, et al. (2000) Detection of preinvasive cancer cells. *Nature* 406: 35-36.
37. Sun Y, Yin Y, Mayers BT, Herricks T, Xia Y (2002) Uniform silver nanowires synthesis by reducing AgNO₃ with ethylene glycol in the presence of seeds and poly (vinyl pyrrolidone). *Chem Mater* 14: 4736-4745.
38. Amani J, Khoshroo A, Rahimi-Nasrabadi M (2018) Electrochemical immunosensor for the breast cancer marker CA 15-3 based on the catalytic activity of a CuS/reduced graphene oxide nanocomposite towards the electrooxidation of catechol. *Microchim Acta*.
39. Nakhjavani SA, Khalilzadeh B, Pakchin PS, Saber R, Ghahremani MH, et al. (2018) A highly sensitive and reliable detection of CA15-3 in patient plasma with electrochemical biosensor labeled with magnetic beads. *Biosens Bioelectron*.